Biomedicine & Pharmacotherapy 134 (2021) 110952

Contents lists available at ScienceDirect

Biomedicine & Pharmacotherapy

journal homepage: www.elsevier.com/locate/biopha

Original article

Mechanistic insights into the intracellular release of doxorubicin from pH-sensitive liposomes

Samara Bonesso dos Reis [a,1], Juliana de Oliveira Silva [b,1], Fernanda Garcia-Fossa [a], Elaine Amaral Leite [b], Angelo Malachias [c], Gwenaelle Pound-Lana [d], Vanessa Carla Furtado Mosqueira [d], Mônica Cristina Oliveira [b], André Luís Branco de Barros [e,**], Marcelo Bispo de Jesus [a,*]

[a] Nano-Cell Interactions Lab., Department Biochemistry & Tissue Biology, Biology Institute, University of Campinas, Campinas, SP, Brazil
[b] Department of Pharmaceutical Products, Faculty of Pharmacy, Federal University of Minas Gerais (UFMG), Belo Horizonte, Minas Gerais, Brazil
[c] Physics Department, Federal University of Minas Gerais (UFMG), Belo Horizonte, Minas Gerais, Brazil
[d] Laboratory of Pharmaceutics and Nanotechnology (LDGNano), Pharmacy School, Federal University of Ouro Preto (UFOP), Minas Gerais, Brazil
[e] Department of Clinical and Toxicological Analyses, Faculty of Pharmacy, Federal University of Minas Gerais (UFMG), Belo Horizonte, Minas Gerais, Brazil

ARTICLE INFO

Keywords:
pH-sensitive liposomes
Doxorubicin
Drug delivery system
Intracellular release

ABSTRACT

pH-sensitive liposomes are interesting carriers for drug-delivery, undertaking rapid bilayer destabilization in response to pH changes, allied to tumor accumulation, a desirable behavior in the treatment of cancer cells. Previously, we have shown that pH-sensitive liposomes accumulate in tumor tissues of mice, in which an acidic environment accelerates drug delivery. Ultimately, these formulations can be internalized by tumor cells and take the endosome-lysosomal route. However, the mechanism of doxorubicin release and intracellular traffic of pH-sensitive liposomes remains unclear. To investigate the molecular mechanisms underlying the intracellular release of doxorubicin from pH-sensitive liposomes, we followed HeLa cells viability, internalization, intracellular trafficking, and doxorubicin's intracellular delivery mechanisms from pH-sensitive (SpHL-DOX) and non-pH-sensitive (nSpHL-DOX) formulations. We found that SpHL-DOX has faster internalization kinetics and intracellular release of doxorubicin, followed by strong nuclear accumulation compared to nSpHL-DOX. The increased nuclear accumulation led to the activation of cleaved caspase-3, which efficiently induced apoptosis. Remarkably, we found that chloroquine and E64d enhanced the cytotoxicity of SpHL-DOX. This knowledge is paramount to improve the efficiency of pH-sensitive liposomes or to be used as a rational strategy for developing new formulations to be applied *in vivo*.

1. Introduction

Nanomedicine employs nanotechnology to prospect for innovative therapeutic tools based on the exclusive properties and performance of nanomaterials. Drug delivery systems (DDS) can change the pharmacokinetics of therapeutics commonly used in medicine, aiming to promote their accumulation in the tumor environment [1]. At least 1055 nanomedicine products have been released to the market [2]; among them, 139 products have been approved by the U.S. Food and Drug Administration (FDA) [3]. Although many of these products aim to treat cancer, multiple barriers prevent the translation of research into the clinic, such as specific delivery into target cells, appropriate intracellular trafficking, and processing [4]. Thus, the application of nanomaterials in medicine requires understanding the mechanisms of intracellular trafficking of DDS into cells.

Among the nanomaterials applied in medicine, liposomes have been widely used due to their capacity to carry both hydrophilic and hydrophobic drugs, and their membrane-like structure that enhances cell

* Corresponding author at: Department of Biochemistry and Tissue Biology, Institute of Biology, University of Campinas - UNICAMP, Rua Monteiro Lobato, 255, Campinas, São Paulo, 13083862, Brazil.
** Corresponding author at: Department of Clinical and Toxicological Analyses, Faculty of Pharmacy, Federal University of Minas Gerais (UFMG), Avenida Antônio Carlos, 6627, Belo Horizonte, Minas Gerais, 31270-910, Brazil.
E-mail addresses: brancodebarros@yahoo.com.br (A.L.B. de Barros), dejesus@unicamp.br (M.B. de Jesus).
[1] These authors contributed equally to this work.

https://doi.org/10.1016/j.biopha.2020.110952
Received 5 August 2020; Received in revised form 21 October 2020; Accepted 27 October 2020
Available online 18 December 2020

affinity and uptake [5]. The PEGylated liposome formulation Doxil® was the first nanomedicine to reach the market in 1995, carrying doxorubicin hydrochloride to treat ovarian cancer and AIDS-related Kaposi's sarcoma cells. Among its clinical improvements, Doxil® leads to a significant reduction of doxorubicin cardiotoxicity and promotes higher drug accumulation inside the tumor [6]. Doxorubicin is effective against many types of solid tumors, and it acts through inhibition of topoisomerase II, preventing DNA replication and inducing apoptosis [7]. As a free drug, doxorubicin accumulates into the cells via passive diffusion, and from its low specificity to cancer cells emerges side effects such as cardiotoxicity, myelosuppression, and mucositis [8]. In contrast, liposomes enter the cells via endocytosis-mediated cellular uptake, providing more specific delivery to tumors [5]. Also, the use of liposomes coated with polyethylene glycol (PEG) prevents its opsonization and subsequent recognition by the reticuloendothelial system, enhancing the circulation and probability to reach the target [9,10]. Therefore, the rational improvement of anticancer therapy will benefit from the detailed knowledge of the interactions between liposomal formulations and cell environment.

One strategy to improve the therapeutic specificity and controlled delivery of drugs is the development of pH-sensitive liposomes (SpHL). This formulation takes advantage of lipid polymorphisms, for example, using protonatable amphiphiles such as cholesteryl hemisuccinate (CHEMS) to stabilize phosphatidylethanolamine (PE) bilayers at physiological pH (~ 7.4). After being internalized by the cells, liposomes take the endocytic route, which travels from early to late endosomes, eventually reaching the lysosomes [11,12]. The drop of intraluminal pH marks this process, and upon acidification within the vesicles, both CHEMS and PE head group protonates and adopt non-lamellar phases such as the hexagonal (H_{II}) one, decreasing the stability of the vesicles that become fusogenic, leading to cytoplasmic leakage of its content [12]. Although most of the data from biochemical assays, including ours, are consistent with this model, a few discrepancies are found when tested *in vitro*. Researches show that some SpHL formulations, composed of DOPE/CHEMS, have a high extent of cell association but low intraluminal pH sensitivity [12]. However, the mechanistic understanding behind intracellular drug release from pH-sensitive liposomes remains unclear. Given the importance of this mechanism for the rational development of more efficient formulations, it is paramount to investigate how these processes drive intracellular drug delivery.

In a previous work, we demonstrated that SpHL carrying doxorubicin (SpHL-DOX) accumulates in mice-breast tumor four times more than non-sensitive pH liposomes (nSpHL-DOX) [13], and that the systemic toxicity of SpHL-DOX was lower than that of free doxorubicin and nSpHL-DOX [14]. Hence, we asked the question, what is the mechanism underlying the intracellular delivery of doxorubicin encapsulated in pH-sensitive liposomes (SpHL-DOX)? To answer this question, we investigated in detail of doxorubicin release from pH-sensitive liposomes using cervical cancer HeLa cells, and the behavior of free doxorubicin (free-DOX) and non-pH-sensitive liposomes containing doxorubicin (nSpHL-DOX) were noted for comparison. We started performing the physicochemical characterization of control liposomes prepared without doxorubicin (SpHL and nSpHL) and formulations containing doxorubicin (SpHL-DOX and nSpHL-DOX). Next, we determined the viability, internalization, intracellular trafficking, and intracellular delivery mechanisms of these formulations and free-DOX. Finally, we investigated the cell death mechanism triggered by DOX encapsulated or not. Understanding the intracellular trafficking and release mechanisms of these formulations is fundamental to improve their therapeutic efficiency.

2. Materials and methods

2.1. Liposome preparation

DOX was purchased from 141 ACIC Chemicals (Brantford, Ontario, Canada). Dioleylphosphatidylethanolamine (DOPE), hydrogenated soy phosphatidylcholine (HSPC), and distearoyl-phosphatidylethanol aminepolyethilenglycol2000 (DSPE-PEG2000) were purchased from the Lipoid GmbH (Ludwigshafen, Germany). Cholesteryl hemisuccinate (CHEMS) and cholesterol (CHOL), 4-(2-Hydroxyethyl)piperazine-1-ethanesulfonic acid (HEPES) salt and ammonium sulphate were supplied by Sigma-Aldrich (St. Louis, USA). Sodium chloride (NaCl) and sodium hydroxide (NaOH) were obtained from Merck (Kenilworth, USA). Policarbonate membranes were purchased from Millipore (Billerica, USA). All other chemicals and reagents were used in analytical grade.

Liposomes were prepared according to the lipid film hydration method previously described by our research group (Silva et al., 2018). Briefly, aliquots of DOPE, CHEMS, and DSPE-PEG2000 or HSPC, CHOL, and DSPE-PEG2000 (5.8: 3.7: 0.5 molar ratio, at 20 mmol L-1 lipid concentration) were transferred to a flask in order to obtain a thin lipid film. NaOH aqueous solution aliquot (equimolar to CHEMS concentration) was added into the flasks containing SpHL thin lipid film in order to promote CHEMS ionization. Then, the flasks were hydrated with ammonium sulphate solution (300 mmol L-1) to form the SpHL or nSpHL. Liposomes size homogenization was performed by extrusion using the Lipex Biomembranes extruder, Model T001 (Vancouver, Canada). After that, ammonium sulphate in the external medium was removed by ultracentrifugation (ultracentrifuge Optima® L-80XP, Beckman Coulter, USA) and 2 mg/mL of DOX was added in SpHL or nSpHL dispersion to remote encapsulation. The non-encapsulated DOX was also removed by ultracentrifugation.

2.2. Cell culture

HeLa cancer cells were grown in 25 or 75 cm^2 culture flasks with DMEM culture medium (Dulbecco's Modified Eagle Medium – Lonza), supplemented with 10 % fetal bovine serum (FBS) (Gibco, Brazil) and 1 % of PenStrep antibiotic (Gibco, Brazil), herein referred as complete medium. During the whole course of experiments, the cells were maintained at 37 °C, with a 5% CO_2 atmosphere in a Panasonic COM-170AICUVL-PA incubator.

2.3. Cell viability with resazurin assay

To evaluate cell viability in the presence of the formulations, HeLa cells (10^4 cells/well) were plated in 96-well plates and incubated for 24 h. After, cells were treated with free-DOX, nSpHL, SpHL, SpHL-DOX, or nSpHL-DOX diluted in serum- and antibiotic-free DMEM medium, and incubated for 6 h, 12 h, or 24 h. Next, the medium was replaced by 100 μL of resazurin (0.015 mg/mL Sigma-Aldrich) diluted in serum and antibiotic-free DMEM medium and incubated for 3 h. Finally, resazurin fluorescence ($\lambda_{ex/em}$ = 560/590 nm) was measured using Cytation 5 Hybrid Multidetection Reader (BioTek Instruments, Inc., Winooski, VT, USA).

2.4. Internalization kinetics

To follow the internalization kinetics of the formulations, HeLa cells (10^5 cells/well) were plated in 12-well plates and incubated for 24 h. The cells were treated with the formulations at their respective IC_{50} concentrations, determined by dose-titration experiments using the

resazurin assay and different times of incubation: 5 min, 15 min, 30 min, 45 min, 1 h, 2 h, 4 h, and 6 h. Subsequently, trypsinized cells were suspended in PBS and analyzed using a FACS Calibur flow cytometer (FACS / Calibur, Becton Dickinson, Mansfield, MA) with an argon ion laser ($\lambda_{ex/em}$ = 488/575 nm / FLH2 channel). The percentage of DOXO-positive cells and the arithmetic means of fluorescence intensities were analyzed using FlowJo™ Software.

2.5. Internalization kinetics in the presence of endocytosis inhibitors

To evaluate the internalization kinetics of the formulations in the presence of endocytosis inhibitors, HeLa cells (10^5 cells/well) were plated in 12-well plates and incubated for 24 h. The cells were pretreated with the endocytosis inhibitors chlorpromazine (10 μM Sigma-Aldrich), Filipin III (20 μM Sigma-Aldrich), and Wortmannin (100 nM Cayman Chemical) for 30 min. Immediately after, cells were treated with the formulations at the respective IC_{50} concentrations, in the presence of the inhibitors, and incubated for 30 min, 1 h, 4 h, and 6 h. The samples were read and analyzed using a FACS Calibur flow cytometer, as described in the previous (1.3) section.

2.6. Cell viability in the presence of endocytosis inhibitors

To establish the contribution of endocytic pathways to the cytotoxicity of the formulations, HeLa cells (10^4 cells/well) were plated in 96-well plates and incubated for 24 h. Cells were pretreated for 30 min with predetermined concentrations of inhibitors: chlorpromazine (10 μM), Filipin III (20 μM), and Wortmannin (100 nM). After 30 min, cells were treated with IC_{50} concentration of each formulation for 6 h and, following the treatment, the medium was replaced by complete medium. After 24 h, cell viability was assessed by resazurin assay as described in section 1.2.

2.7. Intracellular distribution of doxorubicin

To evaluate the intracellular release and intracellular distribution of doxorubicin, HeLa cells (10^5 cells/well) were plated in 12-well plates and incubated for 24 h. Cells were treated with the IC_{50} concentration of each formulation for 6 h, 12 h, and 24 h. After each time point, cells were fixed with paraformaldehyde 4% for 20 min at RT and permeabilized with 0.5 % Triton X-100 for 20 min at RT. Nucleus was counterstained with 1 μg/mL of DAPI (4', 6 diamidino-2-phenylindol, Enzo Life Sciences). Finally, the coverslips were washed thrice with PBS and mounted onto slides with Faramount™ aqueous mounting medium (DAKO, Glostrup, Denmark). Images were acquired using the Leica TCS SP5 II confocal microscope, with 63x objective, 1.0 Airy. Doxorubicin fluorescence ($\lambda_{ex/em}$ = 480/585 nm) was used to image its intracellular distribution. After acquisition, doxorubicin nuclear accumulation was measured by nucleus integrated intensity using a pipeline in CellProfiler 3.0 [15].

2.8. Cell viability in the presence of acidification inhibitors

To understand the contribution of intraluminal acidification to the cytotoxicity of the formulations, HeLa cells (10^4 cells/well) were plated in 96-well plates and incubated for 24 h. Cells were pre-incubated for 30 min with chloroquine (20 μM, Sigma-Aldrich), bafilomycin (0.5 μM, Cayman Chemical), and 3-Methyladenine (2.5 mM, Sigma-Aldrich). After incubation, HeLa cells were treated with the IC_{50} concentration of each formulation for 4 h; then, the medium was replaced by complete medium. After 20 h, cell viability was assessed by resazurin assay, as described in the previous (1.2) section.

2.9. Doxorubicin nuclear accumulation and cell viability in the presence of E64d inhibitor

2.9.1. Doxorubicin intensity

To evaluate the nuclear accumulation of doxorubicin after treatment with E64d, HeLa cells (10^5 cells/well) were plated in 12-well plates and incubated for 24 h. Cells were pre-incubated for 30 min with E64d inhibitor at 10 μM (Sigma-Aldrich). Next, cells were treated with the IC_{50} concentration of each formulation for 6 h, and the treatment was replaced by a complete medium. After 18 h, cells were fixed with 4% paraformaldehyde, permeabilized, and nuclei were counterstained with 1 μg/mL of DAPI (Enzo Life Sciences). Finally, the coverslips were washed thrice with PBS and mounted onto slides with Faramount™ aqueous mounting medium (DAKO, Glostrup, Denmark). Images were acquired using the Leica TCS SP5 II confocal microscope, with 63x objective, 1.0 Airy. Doxorubicin fluorescence ($\lambda_{ex/em}$ = 480/585 nm) was used to image its intracellular distribution using an Argon laser of 488 nm. After acquisition, data were analyzed as described in section 1.6.

2.9.2. Cell viability

To understand the contribution of lysosome proteases to the cytotoxicity of the formulations, HeLa cells (10^4 cells/well) were plated in 96-well plates and grown at the incubator in complete media for 24 h. Cells were pre-incubated for 30 min with E64d inhibitor at 10 μM (Sigma-Aldrich) prior to treatment with each formulation (IC_{50} concentration) in serum- and antibiotic-free medium. After 6 h, the treatment was replaced by a complete medium. After 18 h, viability was assessed by resazurin assay, as described in the previous (1.2) section.

2.10. Cleaved caspases-3 in HeLa cells after treatment by formulations

To assess cleaved caspases-3 activation by the formulations, HeLa cells (10^5 cells/well) were plated on glass coverslips, placed in 12-well plates and grown in complete medium for 24 h. Then, the cells were treated with either free-DOX, SpHL-DOX, or nSpHL-DOX at their respective IC_{50} concentrations for 6 h, 12 h, and 24 h in serum- and antibiotic-free medium. Following the treatments, cells were washed with PBS and fixed with 4% paraformaldehyde for 15 min at 37 °C and permeabilized with 0.1 % Triton X-100 for 5 min at room temperature. Next, cells were washed with PBS and blocked with 10 % FBS in PBS solution for 10 min at room temperature. Subsequently, the coverslips were inverted onto 30 μL drops containing a 1:200 dilution of the cleaved caspase-3 (Asp175) anti-rabbit mAb (Rabbit mAb - Cell Signaling) antibody, for 60 min at 37 °C in a humid chamber. Following incubation, coverslips were washed thrice in blocking solution and incubated with the secondary antibody Alexa Fluor® 647 anti-rabbit IgG (ThermoFisher Scientific, Molecular Probes, Oregon, USA) and nuclei were counterstained with 1 μg/mL of DAPI (Enzo Life Sciences) for 30 min in a humid chamber. Finally, the coverslips were washed thrice with PBS and mounted onto slides with Faramount™ aqueous mounting medium (DAKO, Glostrup, Denmark). Images were acquired using the confocal microscope Leica TCS SP5 II with 63x objective, 1.0 Airy. After acquisition, the cell integrated intensities of cleaved caspases-3 were analyzed with a pipeline in CellProfiler 3.0 [15].

2.11. Statistical analysis

Graphs were plotted using Graph Pad Prism 7.0 Softwares (EUA) where data are represented by the mean ± standard deviation (SD) from three independent experiments carried out in triplicate. Statistical significance was considered when $p < 0.05$. All analyses were subjected to analysis of variance (Two-way ANOVA), followed by Tukey's post-test for analysis of three or more groups, and followed by the Dunnet post-test to compare the different groups with the control group.

3. Results

We started determining the inter-batch variation in the liposomal preparation; the formulations used in this study were characterized according to their physicochemical characterization, pH-sensitivity, fraction of liposomes using liquid chromatography by asymmetric field-flow fractionation (AF4) and liposomes morphology by transmission electron microscopy (TEM). The results (supporting information Table S1 and Figure S1) agree with those obtained by our group in previous studies [13,14].

3.1. Viability of HeLa cells exposed to liposomal formulations: nSpHL and SpHL

The low inter-batch variations enable us to proceed with *in vitro* studies. We started incubating HeLa cells with control liposomes (nSpHL and SpHL) to test whether they have any cytotoxicity. We first evaluated the viability of cells incubated with nSpHL and SpHL (from 0.001 μM to 100 μM) using MTT assay, but we observed viability values around 200 %, which could indicate some interference (supporting information Figure S2A). Liposomal interference in MTT assay might result in an apparent increase of cell viability, because control liposomes themselves may enhance the storage of formazan in cells [16]. Therefore, we decided to assess cell viability by resazurin assay and calcein-AM fluorescence (supporting information, Figure S2B), which showed no interference and revealed that the viability of HeLa cells was unaffected by control liposomes (Fig. 1A) within 24 h. This result rules out the influence of liposomes in the cytotoxicity of formulations containing doxorubicin (*i.e.*, SpHL-DOX and nSpHL-DOX).

Thus, we proceeded to determine the viability of HeLa cells treated with liposomal formulations containing doxorubicin (nSpHL-DOX and SpHL-DOX). For purposes of comparison, we also evaluated the response of the cells to free-DOX. Fig. 1B and supporting information (Fig. 1C) show that SpHL-DOX and free-DOX have comparable cytotoxicity (free-DOX $IC_{50} = 3.2 \pm 1.3$ μM and SpHL-DOX $IC_{50} = 2.1 \pm 0.2$ μM), in good agreement with the literature [17,18]. Conversely, nSpHL-DOX was less cytotoxic, with an approximately 13 times higher ($p < 0.05$) IC_{50} (27.7 ± 9.6 μM). Next, we evaluated cell viability over time after 6 h, 12 h, and 24 h of treatment; we observed that treatments of 6 h and 12 h were not capable of reducing cell viability (no statistical significance of SpHL-DOX and nSpHL-DOX against non-treated cells $p < 0.05$). In contrast, after 24 h, we observed a 50 % reduction in cell viability (Fig. 1C), reaching the IC_{50} observed in the early experiments (Fig. 1B). This result demonstrates that 24 h exposure is required to obtain the cytotoxic effect for free-DOX and liposomal formulations containing DOX. Because we were interested in revealing the underlying mechanism in liposomal delivery and cell death, subsequent experiments were only performed within 24 h.

3.2. Mechanism of internalization and intracellular release of liposomal formulations: nSpHL and SpHL

To investigate the intracellular delivery of doxorubicin by each formulation, we first evaluated the internalization kinetics of the formulations (nSpHL-DOX and SpHL-DOX) following the fluorescence of doxorubicin ($\lambda_{ex/em} = 470/595$ nm) [19]. To compare how each formulation delivered doxorubicin into the cells, we used the same doxorubicin concentration for all formulations, *i.e.*, the IC_{50} of free-DOX (3.22 μM). The internalization (from 5 min up to 6 h) assessed by flow cytometry showed a similar pattern with free-DOX and SpHL-DOX: after 1 h, nearly 100 % of HeLa cells internalized free-DOX and SpHL-DOX (no statistical difference at any time, $p > 0.05$). Meanwhile, nSpHL-DOX required 4 h to reach similar internalizations levels (statistical differences against free-DOX and SpHL-DOX in 1 h, $p < 0.05$) (Fig. 2A). We also calculated the total fluorescence intensity by multiplying the number of positive cells for doxorubicin times the mean fluorescence of doxorubicin [20], a parameter that is proportional to the number of doxorubicin molecules in each positive cell. However, this fluorescent measurement does not consider effects such as fluorescence quenching or enhancement caused by the chemical environment (e.g., DNA binding or self-quenching within the endosomes), thereby it should be interpreted with caution. Nonetheless, this result indicates that even if the same number of cells internalizes free-DOX and SpHL-DOX at 1 h (Fig. 2A), the number of molecules of DOX in free-DOX treated cells is > SpHL > nSpHL-DOX (supporting information Figure S3A). The statistical difference in fluorescence intensity was detected only after 4 h, but free-DOX granted higher fluorescence intensity than the other formulations at this time. To observe if the difference in formulation kinetics was related to the endocytic route, we then studied the endocytic route followed by each formulation.

Pharmacological inhibitors were used to help identify the predominant endocytic pathway for liposomal internalization. The concentration used for each inhibitor was based on the literature, and we tried to minimize their interference in cellular metabolism assessing their cytotoxicity (supporting information Figure S3B). Having determined the ideal inhibitors concentrations, we evaluated the internalization of the formulations by HeLa cells in the presence of inhibitors using flow cytometry. Cells were pretreated with the endocytosis inhibitors for 30 min and then exposed to the formulations IC_{50} for 4 h. As shown in Fig. 2B, none of the inhibitors were capable of reducing the percentage of internalization after 4 h exposure. Small molecules such as free-DOX are expected to enter the cells via passive diffusion [21]; thus no major

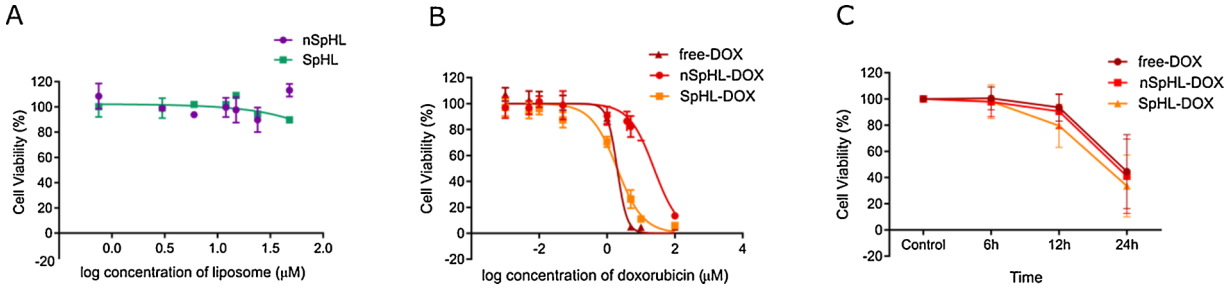

Fig. 1. Viability of HeLa cells treated with free doxorubicin and liposomal formulations in the presence or absence of doxorubicin. (A) Cytotoxicity of empty liposomal formulations containing doxorubicin towards HeLa cancer cells. The cells were treated with non-pH sensitive (nSpHL) and pH-sensitive (SpHL) liposomes diluted in HEPES, in concentrations of 35 μM; 70 μM; 140 μM and 280 μM (lipid concentration). Cell viability was assessed by the resazurin assay. (B) The cells were treated with free-DOX, non-pH-sensitive liposomes (nSpHL-DOX) and pH-sensitive liposomes (SpHL-DOX) both containing doxorubicin and diluted in HEPES, in concentrations of 0.001 μM; 0.05 μM; 1 μM and 100 μM (doxorubicin concentration). (C) Cytotoxicity using the IC_{50} concentrations of doxorubicin treatments at times 6, 12, and 24 h. The cells were treated with nSpHL-DOX and SpHL-DOX, with the IC_{50} concentration of each formulation. Results are expressed as a mean ± standard deviation of three independent experiments (n = 3). Statistical analysis was performed using the Two-Way ANOVA test and multiple comparisons using Tukey's Test. * Significance level $p < 0.05$.

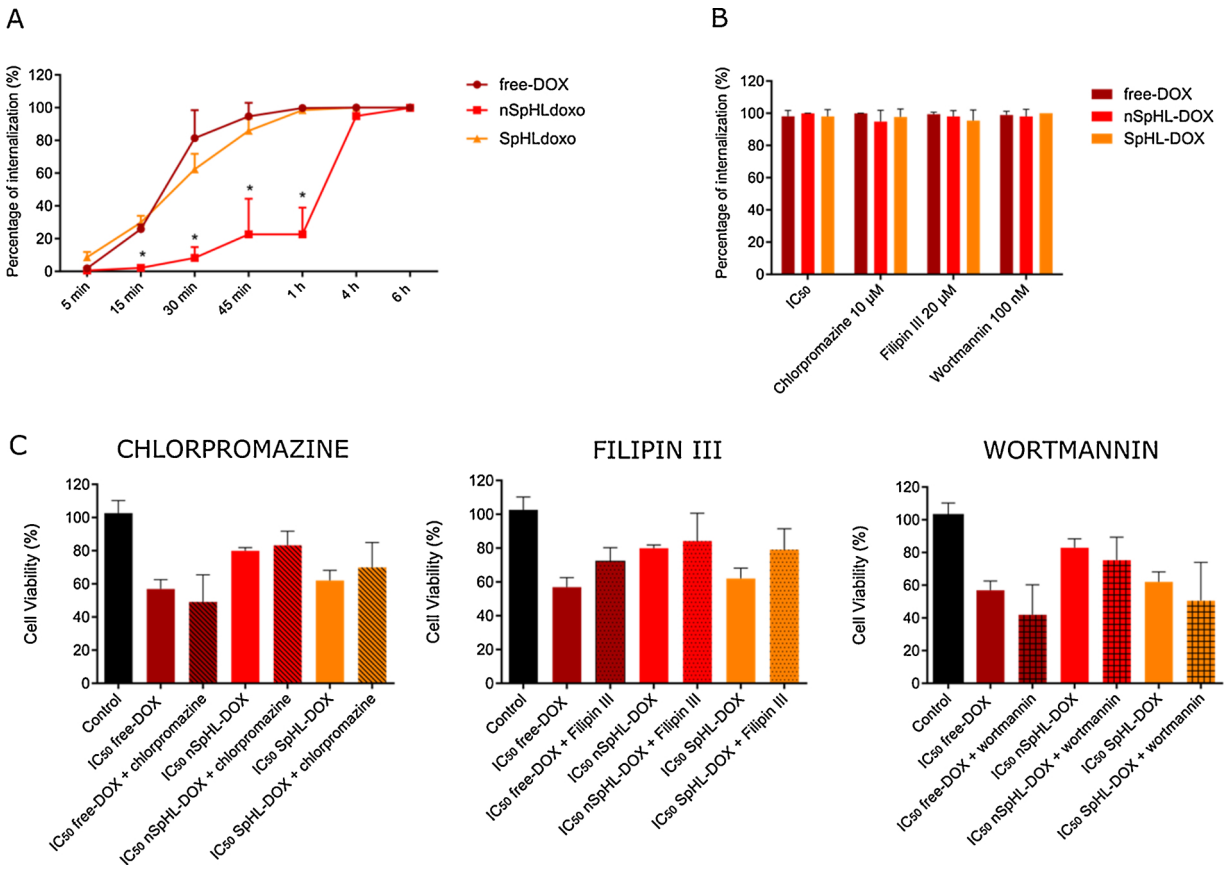

Fig. 2. Effects of formulations on internalization kinetics and endocytosis inhibitors. (A) Internalization kinetics of different formulations over time in HeLa cells. The cells were treated with free-DOX, nSpHL-DOX, and SpHL-DOX for 5 min, 15 min, 30 min, 45 min, 1 h, 2 h, 4 h, and 6 h, and the fluorescence intensity was assessed by flow cytometry. (B) Percentage of internalization of doxorubicin in HeLa cells in the presence of endocytosis inhibitors. The cells were pretreated with the inhibitors (10 μM CPZ, 20 μM FIP and 100 nM WRT) for 30 min, treated with formulations for 4 h and then assessed by flow cytometry. (C) Cell viability of HeLa cells treated with formulations in the presence of endocytosis inhibitors. The cells were pretreated with the inhibitors (10 μM CPZ, 20 μM FIP and 100 nM WRT) for 30 min, and treated with formulations for 6 h, after the incubation time the inhibitors were removed, and the medium was added until 24 h of experiment. Cell viability was assessed by the resazurin assay. Results expressed as mean ± standard deviation of three independent experiments (n = 3). Statistical analysis was performed using the Two-Way ANOVA test and multiple comparisons using Tukey's Test. Significance level *$p <$ 0.05.

inhibition was expected. In contrast, the internalization of liposomes is more likely to occur via endocytosis and converge to the endosome-lysosome route [22,23]. Three hypotheses can explain our results: first, the formulations are internalized by unidentified routes, or second, these cells have compensatory mechanisms, activating one endocytic pathway when another is inhibited, explaining why there is no difference in internalization when one of the endocytic pathways is inhibited [22,24]. Third, the leakage of doxorubicin from liposomes would allow it to freely enter into the cells without being affected by the pharmacological inhibitors.

As the inhibition of endocytosis had no impact on doxorubicin accumulation in HeLa cells, we sought to investigate whether the difference in the endocytic pathway exerted any effect in the cytotoxicity of the formulations. Hence, cells were pretreated with endocytosis inhibitors CPZ, FIP, and WRT, and viability was evaluated after treatment with the respective IC_{50} of free-DOX, SpHL-DOX, or nSpHL-DOX. As observed for internalization, the inhibitors were incapable of decreasing formulations cytotoxicity (no statistical difference, $p <$ 0.05) (Fig. 2C). Different experimental approaches were attempted, but the same results were observed (data not shown). This result indicates that disregarding the endocytic pathways, doxorubicin intracellular accumulation and ultimately its toxicity are inevitable.

After observing that the routes of entry did not explain the differences in the cytotoxicity profile, we investigated how the internalization profile impacted the kinetics of intracellular release of DOX by the formulations. Hence, we treated HeLa cells using the same amount of doxorubicin (IC_{50} of free-DOX) for all the formulations (nSpHL-DOX and SpHL-DOX) to be able to compare the fluorescence intensity among treatments. We evaluated the nuclei accumulation of doxorubicin after 6 h, 12 h, and 24 h using confocal microscopy [25]. After 6 h, free-DOX was already accumulated in the nuclei, as expected for a drug that enters the cell via passive diffusion. Interestingly, SpHL-DOX led to higher nuclear accumulation of doxorubicin than free-DOX at 6 h (statistical difference III, $p <$ 0.05). As demonstrated in internalization studies, nSpHL-DOX led to lower accumulation of doxorubicin and the fluorescence signal was similarly distributed throughout the first 12 h, leading to a minor accumulation of doxorubicin only after 24 h (Fig. 3). These results suggest SpHL-DOX has a faster intracellular release when compared to nSpHL-DOX but promoted sustained release if compared to free-DOX. DOPE-based liposomes are more avidly internalized by cells, in particular when using the DOPE/CHEMS blend. The low degree of hydration of the DOPE together with the small head group of CHEMS result in a loosely packed bilayer, which is claimed to favor the interaction with the cell membrane, thereby facilitating internalization [26,27].

3.3. *Intracellular trafficking: the effect of intraluminal pH in the release of doxorubicin*

Acidification inhibitors were used to help identify the role of

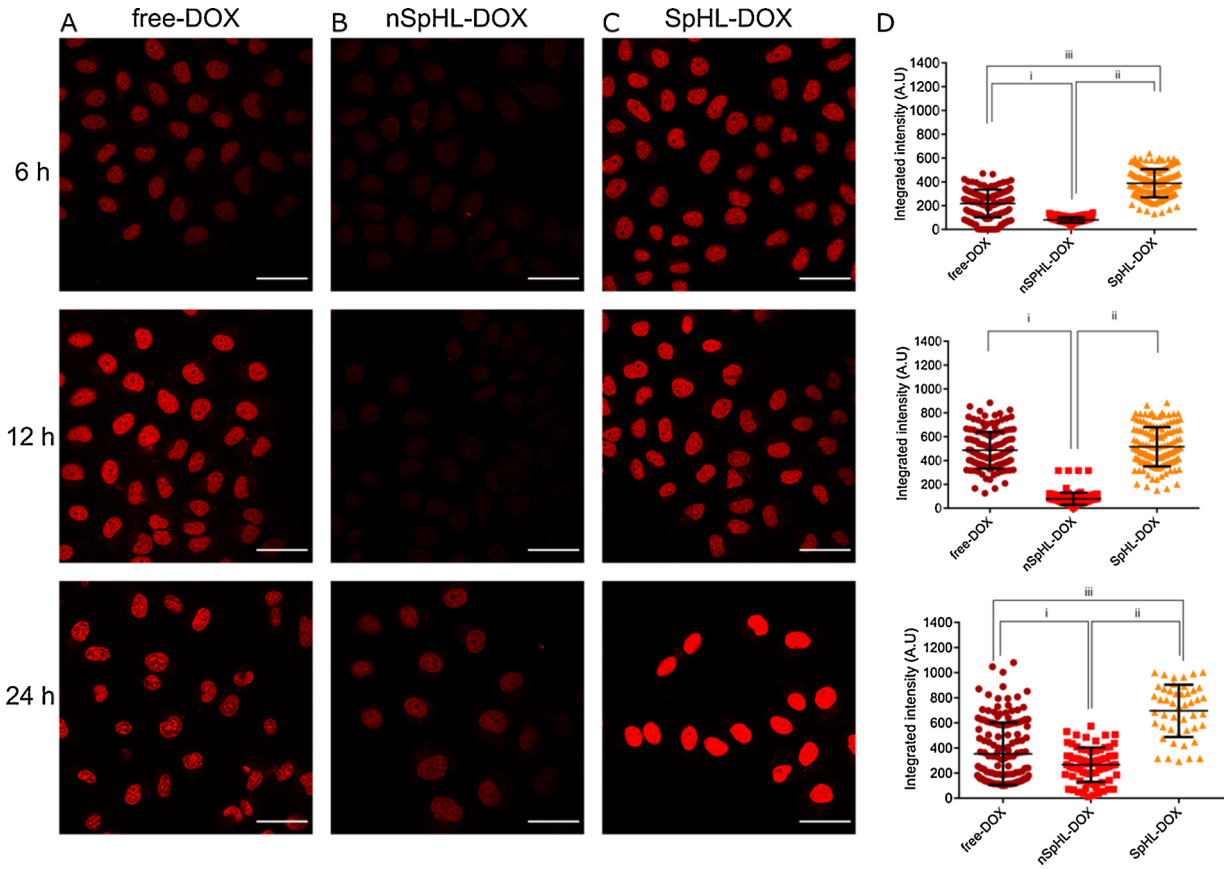

Fig. 3. Intracellular delivery of doxorubicin measured by its nuclear accumulation in HeLa cells. The cells were treated with the IC_{50} (3.22 μM) of free-DOX for all formulations in order of comparison. After the 24 h, the coverslips were fixed and, subsequently, the images were acquired with a 63x objective using confocal microscopy. Integrated intensity in the nuclei is reported for 6 h, 12 h, and 24 h. Results expressed as median ± standard deviation of three independent experiments (n = 3). Statistical analysis was performed using the Two-Way ANOVA test and multiple comparisons using the Tukey's Test. Significance level $*p < 0.05$, where (i) significant difference between free-DOX and nSpHL-DOX; (ii) significant difference between SpHL-DOX and nSpHL-DOX; and (iii) significant difference between free-DOX and SpHL-DOX. Scale bar = 100 μm.

intraluminal pH in the release of doxorubicin from the liposomal formulations. The concentration of each inhibitor used was based on the literature, and before using them, we have determined their cytotoxicity and effectiveness in inhibiting lysosomal acidification (supporting information Figure S4). To understand the contribution of vesicle acidification to the release of DOX, we pretreated the cells with the inhibitors for 4 h, and then the cells were treated with the IC_{50} concentration of each formulation, free-DOX, SpHL-DOX, and nSpHL-DOX for 24 h. 3-MA and BAF did not affect the toxicity profile of the formulations, while CLQ increased the cytotoxicity of SpHL-DOX (Fig. 4A).

Proteases such as cathepsins are essential to the appropriate function of the lysosome route and autolysosome formation, which in turn is essential to cellular homeostasis [28]. To test whether lysosomal proteases were coupled to the SpHL-DOX increase in cytotoxicity, we used the E64d membrane-permeable inhibitor, which inhibits cathepsins B, H, and L, and leads to impairment of autophagy [29]. We pretreated the cells with E64d followed by 6 h treatment with free-DOX and liposomal formulations. We observed that the integrated intensity of DOX in the nuclei was enhanced for free-DOX and SpHL-DOX when cells are pretreated with E64d, but not for nSpHL (Fig. 4B). This result reveals that when cathepsins in the lysosome are inhibited, free-DOX and SpHL-DOX have their release, and subsequently, nuclear accumulation increased. This increase reflected in cell viability: doxorubicin cytotoxicity was increased in the presence of E64d. The effect was about 1.4 times higher for free-DOX, 2.5 times for nSpHL-DOX, and 6.5 times for SpHL-DOX (Fig. 4C), being particularly important for SpHL-DOX. One hypothesis is that a percentage of SpHL-DOX, in the absence of the inhibitor, is entrapped in the lysosome, and perturbations in the lysosome may enhance the release of DOX and consequently its cytotoxicity. Another hypothesis is that SpHL releases DOX prior to lysosomal acidification at the endosome stage, but further investigations would be necessary to identify the role of autophagy in this process.

3.4. Caspase-3 induced-apoptosis in HeLa cells by release of DOX

Doxorubicin is known for triggering cell death through activation of caspases and subsequent apoptosis [30]. Caspase-3 catalyzes the cleavage of cellular proteins to activate the apoptotic program, and its activation may be dependent on cytochrome c release and caspase-9, leading to caspases-3 cleavage [31]. Given the different profiles in the intracellular release of doxorubicin, we sought to confirm the positive correlation between the nuclear accumulation of doxorubicin and the activation of caspases-3 by our formulations. Cells were treated with the formulations for 6 h, 12 h and 24 h using the IC_{50} of free-DOX, and immunostained for cleaved caspase-3. The intensity of cleaved caspases-3 from confocal images was analyzed by the single-cell method using CellProfiler [15], which brought robustness to the results. Our results confirmed that after 6 h and 12 h, free-DOX treated cells had higher integrated intensity of the protein than SpHL-DOX and nSpHL-DOX (statistical difference, $p < 0.05$); this activation decreased after 24 h. At 12 h a mild activation of cleaved caspase-3 by nSpHL-DOX was observed, which was absent after 24 h. Interestingly, SpHL-DOX activated cleaved caspase-3 after 12 h, and this activation was still at high levels after 24 h. Both formulations, free-DOX and SpHL-DOX,

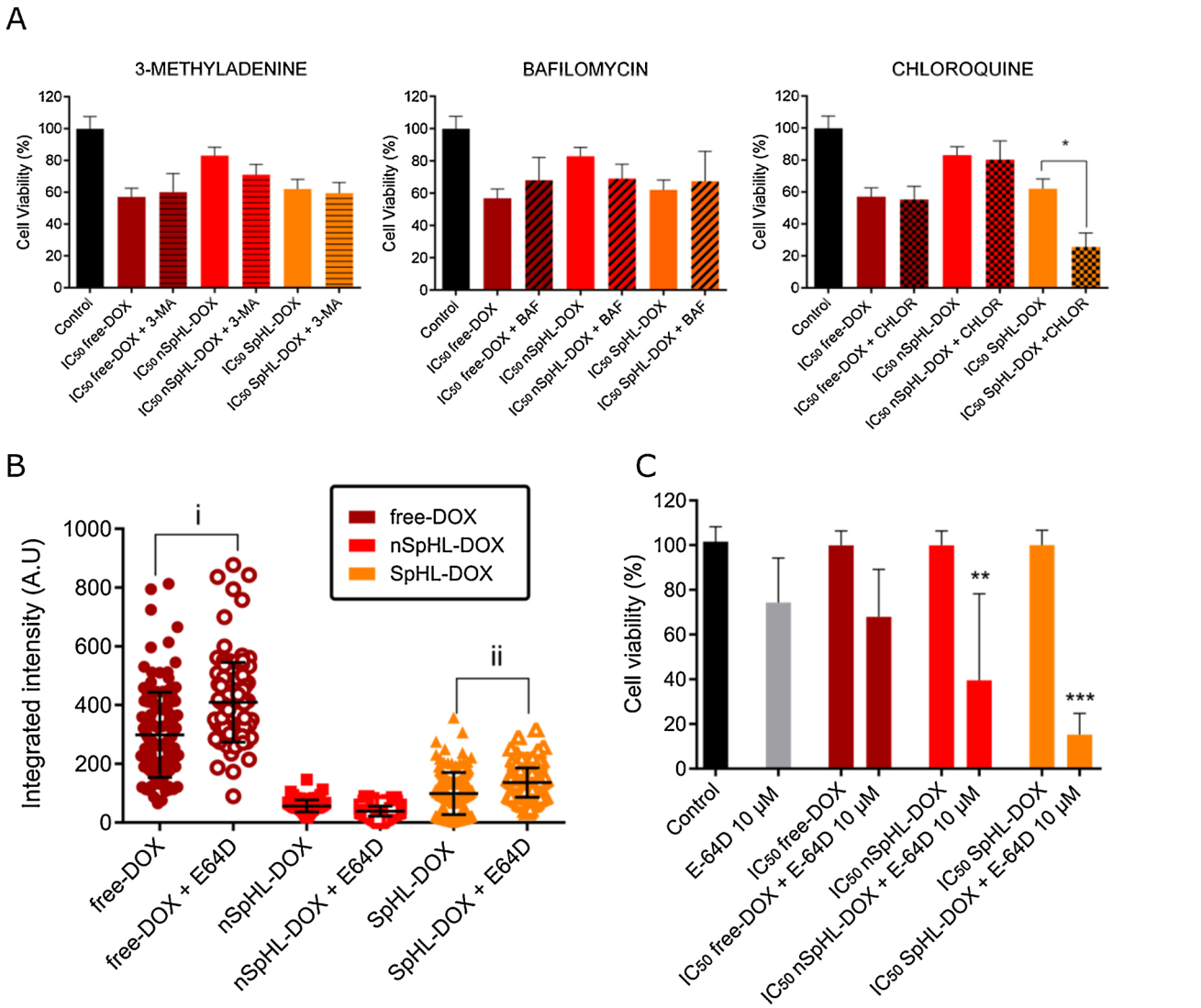

Fig. 4. Acidic vesicles inhibitors and effects of formulations carrying doxorubicin. (A) Cell viability of HeLa cells in the presence of endosomal acidification inhibitors 2.5 mM 3-MA, 0.5 µM BAF, and 20 µM CLQ. The cells were incubated for 4 h. After the incubation, inhibitors were removed, and the medium was added, until completing 24 h. After 24 h, viability was assessed by the resazurin assay. The control group without inhibitor was considered as 100 % of the cells in cell viability. (B) Pretreatment with E-64d for 30 min, and then cells were treated for 6 h with the formulations. Then, single-cell analysis with CellProfiler analyzed the integrated intensity of DOX in the nuclei. (C) Cell viability after pretreatment with E-64d during 30 min, and then cells were treated for 6 h with the formulations. After the incubation, E64d was removed, and the medium was added, until completing 24 h. Then, cell viability was assessed with resazurin assay. For statistical analysis in (B), was performed using One-Way ANOVA test followed by Tukey's test; (i) significant difference between free-DOX and free-DOX + E64d and (ii) SpHL-DOX and SpHL-DOX + E64d. For the analysis in (C), each formulation without E64d was considered 100 %. All treatments were compared with E64d 10 µM; ** nSpHL-DOX + E64d vs E64d and *** SpHL-DOX + E64d vs E64d. Results expressed as mean ± standard deviation of three independent experiments (n = 3). Statistical analysis was performed using One-Way ANOVA test with post-test of multiple Bonferroni's analyzes. Significance level *$p < 0.05$.

induced activation of cleaved caspase-3 at the same levels after 24 h (no significant difference, $p < 0.05$) (Fig. 5). Overall, our results confirmed the positive correlation between nuclear accumulation of doxorubicin and caspase-3 activation.

4. Discussion

In this work, we tackled the following question: what is the mechanism underlying the intracellular delivery of doxorubicin encapsulated in pH-sensitive liposomes (SpHL-DOX) into HeLa cells? Despite the similarities in IC_{50} values and internalization kinetics between SpHL-DOX and doxorubicin, our main findings revealed that SpHL-DOX toxicity enhanced when lysosome acidification was inhibited using chloroquine and lysosome proteases are inhibited using E64d. To the best of our knowledge, it is the first time these processes positively correlate with the intracellular release of drugs from pH-sensitive liposomes. Thus, our data support the hypothesis that at the intracellular level, pH seems to play a secondary role in the release of cargo from some pH-sensitive liposomal formulations and suggest that instead of the cargo, in this case, doxorubicin can play an important role in controlling its own release.

The use of lysosomotropic and intracellular trafficking perturbating agents alludes to the idea that interfering in the intracellular trafficking of pH-sensitive liposomes could lead to improved drug release. The presence of lysosomotropic agents (*e.g.*, chloroquine, bafilomycin A, and 3-MA) typically prevents intracellular release of fluorophores (*e.g.*, calcein, FITC-dextran) and biologically relevant cargos (*e.g.*, drugs, plasmid DNA) from pH-sensitive liposomes [32,33]. The release is prevented by the dissipation of the intraluminal pH, which in turn avoids PE phase transition and thereby lipid fusion. Conversely, no appreciable decrease

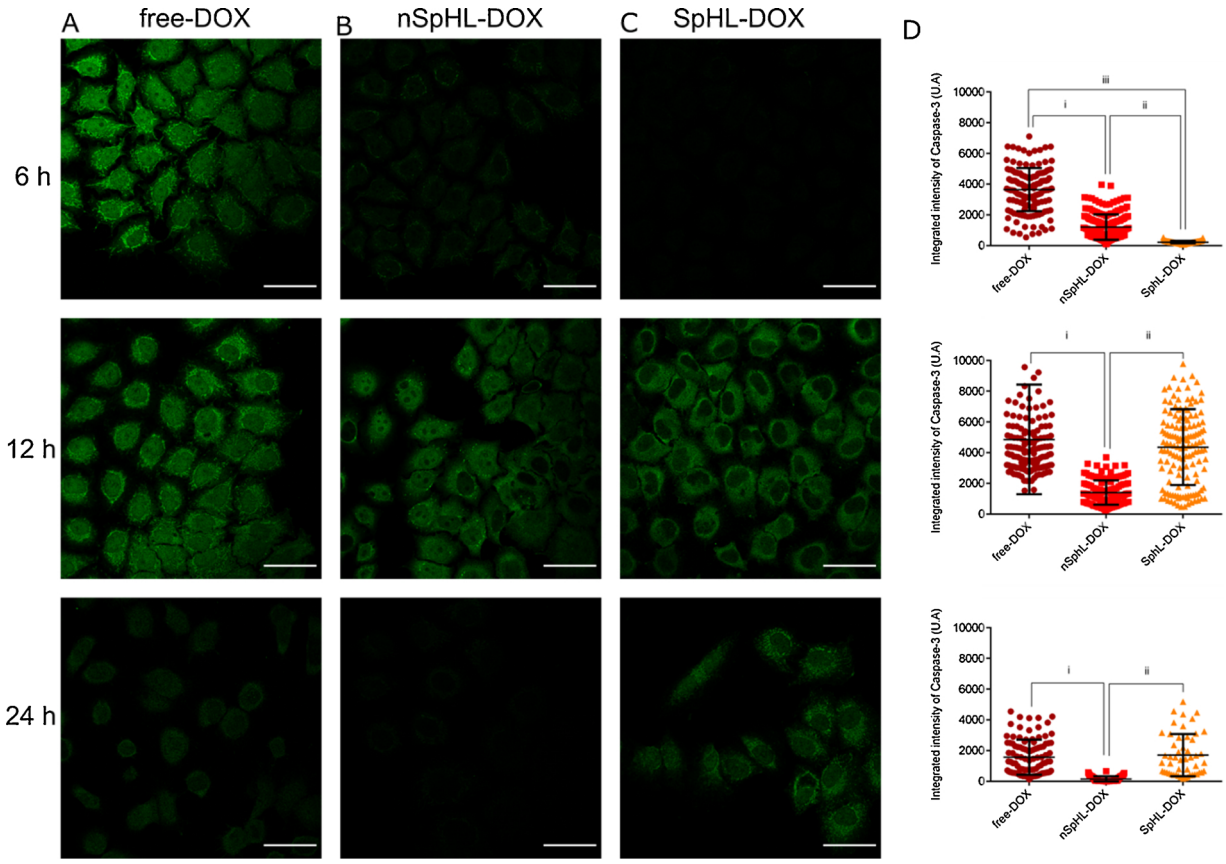

Fig. 5. Immunocytochemistry of cleaved caspase-3 protein in HeLa cells after treatment with the formulations. Cells were treated with free-DOX, nSpHL-DOX, and SpHL-DOX with 3.22 μM (IC_{50} of free-DOX), for 6, 12, and 24 h. After, the coverslips were fixed with 4% PFA and subsequently labeled with cleaved caspase-3 (Asp175) anti-rabbit mAb. Then, coverslips were incubated with the secondary antibody Alexa Fluor® 647 anti-rabbit IgG. (A) Representative images of the HeLa cell with green representing cleaved caspase-3. (B) Cells' integrated intensity of cleaved caspase-3 from the treatments with the formulations. Results expressed as median ± standard deviation of three independent experiments (n = 3). Statistical analysis was performed using the Two-Way ANOVA test and multiple comparisons using Tukey's Test. Significance level $*p < 0.05$, where (i) significant difference between free-DOX and nSpHL-DOX; (ii) significant difference between SpHL-DOX and nSpHL-DOX; and (iii) significant difference between free-DOX and SpHL-DOX. Scale bar =100 μm.

in doxorubicin release was observed in response to SpHL-DOX in the presence of bafilomycin and 3-MA. In fact, chloroquine further increased doxorubicin cytotoxicity. It is tempting to hypothesize that chloroquine could be potentializing cell toxicity by inhibiting autophagy, P-glycoprotein, DNA repair, or even upregulate p53-mediated apoptosis; however, this hypothesis is weakened by the fact that this increase was not observed with free-DOX, nSpHL-DOX, nor in the presence of 3-MA, another autophagic inhibitor. We, therefore, hypothesize that the presence of chloroquine inside the intraluminal vesicle triggers doxorubicin release from SpHL-DOX, probably by osmotic swelling and disruption of the endosome [34]. Previous studies found that the decrease in pH is not the only mechanism that leads to destabilization of pH-sensitive liposomes inside the cell, even though biophysical assays show a clear correlation between acidic pH and liposomes rupture [27,35]. The increased toxicity of SpHL-DOX in the presence of E64d could be related to doxorubicin's higher nuclear accumulation. Even in the absence of inhibitor, SpHL-DOX leads to higher accumulation of doxorubicin in nuclei compared to free-DOX and nSpHL-DOX; this effect is intensified in the presence of E64d. A likely explanation is that entrapped drugs in acidic vesicles can be released by decreasing the pH gradient along the endocytic route using inhibitors [36]. These findings suggest that the release from pH-sensitive liposomes containing doxorubicin involves more complex mechanisms than simply the decrease of the intraluminal pH.

The role of the cargo in the intracellular release is rarely taken into consideration during the development of DDS, but as presented here, it may constitute a key element to trigger endosomal destabilization, particularly in the presence of perturbating agents. Encapsulation into liposomes is an alternative to diminish the side effects related to doxorubicin free circulation such as cardiotoxicity, myelosuppression, and mucositis [8]. We previously demonstrated that both nSpHL-DOX and SpHL-DOX accumulate in mice-breast tumors, the latter being four-fold higher than the former [13], and SpHL-DOX led to reduced systemic toxicity compared to free-DOX and nSpHL-DOX [14]. The biodistribution throughout the mice showed higher accumulation of nSpHL-DOX into the liver and spleen than SpHL-DOX, which accumulated at higher concentrations into the tumor than nSpHL-DOX. This difference could be explained by the structural lipid used to produce nSpHL (HSPC), improving the liposome recognition by the mononuclear phagocyte system and reducing its bioavailability [13]. Thus, an improvement in SpHL-DOX toxicity towards cancer cells is desirable for *in vivo* applications [37], and a remarkable finding here is that combining chloroquine or E64d with SpHL-DOX enhanced the intracellular release of the drug, its capacity of triggering apoptosis resulting in a greater toxicity. These promising results, allied with our previous *in vivo* findings, encourage further studies to assess the real potential of these therapeutic strategies *in vivo*.

Our work highlights the importance of studying in a mechanistic way the route for the release of doxorubicin by the formulations, and it opens new opportunities to develop and improve the formulations. New hypotheses emerge for further *in vivo* and *in vitro* studies, which could help to elucidate the role of autophagy in the intracellular trafficking process. Autophagy is a process induced in response to extracellular and intracellular stress for the turnover of cellular components, and it could be

deregulated during disease progression [29]. Cathepsin B expression levels appear significantly elevated in some types of cancer, and this protein was described to be activated in doxorubicin-mediated cell death [38]. Inhibitors of acidification such as chloroquine, or inhibitors of lysosomal cathepsins like E64d block the degradation of proteins related to autophagy and lead to accumulation of LC3-II [39]. Studies are now needed to further investigate these hypotheses.

5. Conclusion

This work highlights that SpHL-DOX release of doxorubicin outperforms that of free doxorubicin and nSpHL-DOX in inducing the expression of cleaved caspase-3. Remarkably, SpHL-DOX potency was further increased in the presence of chloroquine and E64d, opening new opportunities for improvement of its therapeutic application. From the drug delivery perspective, we showed that the cargo (*i.e.*, doxorubicin) can play a key role in its release from pH-sensitive liposomes, suggesting a more complex mechanism than simply a decrease of the intraluminal pH. This mechanistic knowledge could be useful for improving or developing a new formulation containing DOX. From the cancer cell biology perspective, future studies will be needed to determine the role of autophagy in the intracellular pathway of such formulations, also as a possible strategy for improving liposomal formulations efficiency.

Declaration of Competing Interest

The authors declare that there are no conflicts of interest.

Acknowledgements

This research was supported by FAEPEX (process 3097/17), São Paulo Research Foundation (FAPESP, Grants #2014/03002-7 and #2015/06134-4), and National Council for Scientific and Technological Development (CNPq, Grants #429703/2018-0). Authors thank the fellowships provided to S.B.R. by the Coordination for the Improvement of Higher Education Personnel (CAPES) and to M.B.J, A.L.B.B, A.M., V.C.F. M., and M.C.O. by the National Council for Scientific and Technological Development (CNPq). We also thank E. de Paula and J. M. Nascimento for their feedback and comments on review of this manuscript. We would like to thank the Brazilian Synchrotron Light Laboratory (LNLS) for their financial support and assistance in the SAXS acquisition and the Center of Microscopy at UFMG for the assistance in the TEM analysis.

Appendix A. Supplementary data

Supplementary material related to this article can be found, in the online version, at doi:https://doi.org/10.1016/j.biopha.2020.110952.

References

[1] D.J. Irvine, E.L. Dane, Enhancing cancer immunotherapy with nanomedicine, Nat. Rev. Immunol. 20 (2020) 321–334, https://doi.org/10.1038/s41577-019-0269-6.
[2] StatNano, StatNano, 2020 (accessed May 12, 2020), https://product.statnano.com//industry/medicine.
[3] A.-A.D. Jones, G. Mi, T.J. Webster, A status report on FDA approval of medical devices containing nanostructured materials, Trends Biotechnol. 37 (2019) 117–120, https://doi.org/10.1016/j.tibtech.2018.06.003.
[4] R. van der Meel, E. Sulheim, Y. Shi, F. Kiessling, W.J.M. Mulder, T. Lammers, Smart cancer nanomedicine, Nat. Nanotechnol. 14 (2019) 1007–1017, https://doi.org/10.1038/s41565-019-0567-y.
[5] A. Gao, X. Hu, M. Saeed, B. Chen, Y. Li, H. Yu, Overview of recent advances in liposomal nanoparticle-based cancer immunotherapy, Acta Pharmacol. Sin. 40 (2019) 1129–1137, https://doi.org/10.1038/s41401-019-0281-1.
[6] U. Bulbake, S. Doppalapudi, N. Kommineni, W. Khan, Liposomal formulations in clinical use: an updated review, Pharmaceutics 9 (2017), https://doi.org/10.3390/pharmaceutics9020012.
[7] H. Taymaz-Nikerel, M.E. Karabekmez, S. Eraslan, B. Kırdar, Doxorubicin induces an extensive transcriptional and metabolic rewiring in yeast cells, Sci. Rep. 8 (2018) 13672, https://doi.org/10.1038/s41598-018-31939-9.
[8] P. Liang, D. Zhao, C.-Q.-Q. Wang, J.-Y.-Y. Zong, R.-X.-X. Zhuo, S.-X.-X. Cheng, Facile preparation of heparin/CaCO3/CaP hybrid nano-carriers with controllable size for anticancer drug delivery, Colloids Surf. B Biointerfaces 102 (2013) 783–788, https://doi.org/10.1016/j.colsurfb.2012.08.056.
[9] I. Sugiyama, Y. Sadzuka, Characterization of novel mixed polyethyleneglycol modified liposomes, Biol. Pharm. Bull. 30 (2007) 208–211, https://doi.org/10.1248/bpb.30.208.
[10] S.S. Nunes, R.S. Fernandes, C.H. Cavalcante, I. da Costa César, E.A. Leite, S.C. A. Lopes, et al., Influence of PEG coating on the biodistribution and tumor accumulation of pH-sensitive liposomes, Drug Deliv. Transl. Res. 9 (2019) 123–130, https://doi.org/10.1007/s13346-018-0583-8.
[11] H. Karanth, R.S.R. Murthy, pH-Sensitive liposomes - Principle and application in cancer therapy, J. Pharm. Pharmacol. 59 (2007) 469–483, https://doi.org/10.1211/jpp.59.4.0001.
[12] S.R. Paliwal, S.R. Paliwal, S.P. Vyas, A review of mechanistic insight and application of pH-sensitive liposomes in drug delivery, Drug Deliv. 22 (2015) 231–242, https://doi.org/10.3109/10717544.2014.882469.
[13] J.O. Silva, R.S. Fernandes, S.C.A. Lopes, V.N. Cardoso, E.A. Leite, G.D. Cassali, et al., pH-sensitive, long-circulating liposomes as an alternative tool to deliver doxorubicin into tumors: a feasibility animal study, Mol. Imaging Biol. 18 (2016) 898–904, https://doi.org/10.1007/s11307-016-0964-7.
[14] J. de Oliveira Silva, S.E.M. Miranda, E.A. Leite, A. de Paula Sabino, K.B.G. Borges, V.N. Cardoso, et al., Toxicological study of a new doxorubicin-loaded pH-sensitive liposome: a preclinical approach, Toxicol. Appl. Pharmacol. 352 (2018) 162–169, https://doi.org/10.1016/j.taap.2018.05.037.
[15] C. McQuin, A. Goodman, V. Chernyshev, L. Kamentsky, B.A. Cimini, K.W. Karhohs, et al., CellProfiler 3.0: Next-generation image processing for biology, PLoS Biol. 16 (2018), e2005970, https://doi.org/10.1371/journal.pbio.2005970.
[16] F. Angius, A. Floris, Liposomes and MTT cell viability assay: an incompatible affair, Toxicol. In Vitro 29 (2015) 314–319, https://doi.org/10.1016/j.tiv.2014.11.009.
[17] M. Alyane, G. Barratt, M. Lahouel, Remote loading of doxorubicin into liposomes by transmembrane pH gradient to reduce toxicity toward H9c2 cells, Saudi Pharm. J. 24 (2016) 165–175, https://doi.org/10.1016/j.jsps.2015.02.014.
[18] J.G. Rosch, A.L. Brown, A.N. DuRoss, E.L. DuRoss, G. Sahay, C. Sun, Nanoalginates via Inverse-Micelle Synthesis: Doxorubicin-Encapsulation and Breast Cancer Cytotoxicity, Nanoscale Res. Lett. 13 (2018) 350, https://doi.org/10.1186/s11671-018-2748-2.
[19] N.S.H. Motlagh, P. Parvin, F. Ghasemi, F. Atyabi, Fluorescence properties of several chemotherapy drugs: doxorubicin, paclitaxel and bleomycin, Biomed. Opt. Express 7 (2016) 2400–2406, https://doi.org/10.1364/BOE.7.002400.
[20] O. Mizrahi, E.I. Shalom, M. Baniyash, Y. Klieger, Quantitative Flow Cytometry: Concerns and Recommendations in Clinic and Research, Cytometry B Clin. Cytom. 94 (2018) 211–218, https://doi.org/10.1002/cyto.b.21515.
[21] X. Zeng, R. Morgenstern, A.M. Nyström, Nanoparticle-directed sub-cellular localization of doxorubicin and the sensitization breast cancer cells by circumventing GST-Mediated drug resistance, Biomaterials 35 (2014) 1227–1239, https://doi.org/10.1016/j.biomaterials.2013.10.042.
[22] M.B. de Jesus, Y.L. Kapila, Cellular mechanisms in nanomaterial internalization, intracellular trafficking, and toxicity, in: N. Durán, S.S. Guterres, O.L. Alves (Eds.), Nanotoxicology Mater. Methodol. Assess., Springer, New York, NY, 2014, pp. 201–227, https://doi.org/10.1007/978-1-4614-8993-1_9.
[23] Y. Li, L. Gao, X. Tan, F. Li, M. Zhao, S. Peng, Lipid rafts-mediated endocytosis and physiology-based cell membrane traffic models of doxorubicin liposomes, Biochim. Biophys. Acta BBA – Biomembr. 1858 (2016) 1801–1811, https://doi.org/10.1016/j.bbamem.2016.04.014.
[24] G.J. Doherty, H.T. McMahon, Mechanisms of endocytosis, Annu. Rev. Biochem. 78 (2009) 857–902, https://doi.org/10.1146/annurev.biochem.78.081307.110540.
[25] C. Wang, C. Wu, X. Zhou, T. Han, X. Xin, J. Wu, et al., Enhancing Cell Nucleus Accumulation and DNA Cleavage Activity of Anti-Cancer Drug via Graphene Quantum Dots, Sci. Rep. 3 (2013) 1–8, https://doi.org/10.1038/srep02852.
[26] C.-J.-J. Chu, J. Dijkstra, M.-Z.-Z. Lai, K. Hong, F.C. Szoka, Efficiency of cytoplasmic delivery by pH-Sensitive liposomes to cells in culture, Pharm. Res. 7 (1990) 824–834, https://doi.org/10.1023/A:1015908831507.
[27] S. Simões, V. Slepushkin, N. Düzgünes, M.C. Pedroso de Lima, On the mechanisms of internalization and intracellular delivery mediated by pH-sensitive liposomes, Biochim. Biophys. Acta BBA - Biomembr 1515 (2001) 23–37, https://doi.org/10.1016/S0005-2736(01)00389-3.
[28] M. Jung, J. Lee, H.-Y.-Y. Seo, J.S. Lim, E.-K.-K. Kim, Cathepsin inhibition-induced lysosomal dysfunction enhances pancreatic beta-cell apoptosis in high glucose, PLoS One 10 (2015), e0116972, https://doi.org/10.1371/journal.pone.0116972.
[29] Y. Yang, L. Hu, H. Zheng, C. Mao, W. Hu, K. Xiong, et al., Application and interpretation of current autophagy inhibitors and activators, Acta Pharmacol. Sin. 34 (2013) 625–635, https://doi.org/10.1038/aps.2013.5.
[30] F. Brisdelli, M. Perilli, D. Sellitri, P. Bellio, A. Bozzi, G. Amicosante, et al., Protolichesterinic acid enhances doxorubicin-induced apoptosis in HeLa cells in vitro, Life Sci. 158 (2016) 89–97, https://doi.org/10.1016/j.lfs.2016.06.023.
[31] M.A. Eldeeb, R.P. Fahlman, M. Esmaili, M.A. Ragheb, Regulating Apoptosis by Degradation: The N-End Rule-Mediated Regulation of Apoptotic Proteolytic Fragments in Mammalian Cells, Int. J. Mol. Sci. 19 (2018) 3414, https://doi.org/10.3390/ijms19113414.
[32] J. Connor, L. Huang, pH-sensitive Immunoliposomes as an Efficient and Target-specific Carrier for Antitumor Drugs, Cancer Res. 46 (1986) 3431–3435.
[33] M.P. Wehunt, C.A. Winschel, A.K. Khan, T.L. Guo, G.R. Abdrakhmanova, V. Sidorov, Controlled drug-release system based on pH-sensitive chloride-triggerable liposomes, J. Liposome Res. 23 (2013) 37–46, https://doi.org/10.3109/08982104.2012.727423.

[34] L. Qiu, N. Jing, Y. Jin, Preparation and in vitro evaluation of liposomal chloroquine diphosphate loaded by a transmembrane pH-gradient method, Int. J. Pharm. 361 (2008) 56–63, https://doi.org/10.1016/j.ijpharm.2008.05.010.
[35] Z. Vanić, S. Barnert, R. Süss, R. Schubert, Fusogenic activity of PEGylated pH-sensitive liposomes, J. Liposome Res. 22 (2012) 148–157, https://doi.org/10.3109/08982104.2011.633267.
[36] C.M. Lee, I.F. Tannock, Inhibition of endosomal sequestration of basic anticancer drugs: influence on cytotoxicity and tissue penetration, Br. J. Cancer 94 (2006) 863–869, https://doi.org/10.1038/sj.bjc.6603010.
[37] X. Gao, T. Yu, G. Xu, G. Guo, X. Liu, X. Hu, et al., Enhancing the anti-glioma therapy of doxorubicin by honokiol with biodegradable self-assembling micelles through multiple evaluations, Sci. Rep. 7 (2017) 43501, https://doi.org/10.1038/srep43501.
[38] S. Bien, C. Rimmbach, H. Neumann, J. Niessen, E. Reimer, C.A. Ritter, et al., Doxorubicin-induced cell death requires cathepsin B in HeLa cells, Biochem. Pharmacol. 80 (2010) 1466–1477, https://doi.org/10.1016/j.bcp.2010.07.036.
[39] N. Mizushima, T. Yoshimori, B. Levine, Methods in mammalian autophagy research, Cell 140 (2010) 313–326, https://doi.org/10.1016/j.cell.2010.01.028.